# Thermal Simulations of a New SiC Detector Design for Neutron Measurements in JSI Nuclear Research Reactor

Valentin Valero[1,a*], Laurent Ottaviani[1,b], Abdallah Lyoussi[2,c],
Vladimir Radulović[3,d], Luka Snoj[3,e], Adrien Volte[1,f], Michel Carette[1,g]
and Christelle Reynard-Carette[1,h]

[1]Aix Marseille Univ, Université de Toulon, CNRS, IM2NP, Marseille, France

[2]CEA/DES/IRESNE/DER, Section of Experimental Physics, Safety Tests and Instrumentation, Cadarache, F-13108, Saint Paul-lez-Durance, France

[3]Reactor Physics Division, Jožef Stefan Institute, Ljubljana, Slovenia

[a]valentin.valero@im2np.fr, [b]laurent.ottaviani@im2np.fr, [c]abdallah.lyoussi@cea.fr,
[d]vladimir.radulovic@ijs.si, [e]luka.snoj@ijs.si, [f]adrien.volte@univ-amu.fr, [g]michel.carette@univ-amu.fr, [h]christelle.carette@univ-amu.fr

**Keywords:** Silicon Carbide, semiconductors, neutrons, detector, 3D thermal simulations.

**Abstract.** Today, to respond to the increase of development of accurate, precise and relevant experiments in nuclear research reactors and tokamaks with their severe and intense operating conditions, there is a major need of innovative sensors that can accurately measure key parameters such as neutron and photon fluxes or nuclear heating rates. Thus, innovation in the field of nuclear instrumentation and measurements is a privileged research topic. It is crucial to develop optimized devices for accurate on-line in-core measurements, and scientific/technological requirements for various applications such as ageing of materials, safety applications, beam monitoring or nuclear physics. Nowadays, more and more semiconductors are used as sensor materials in nuclear instrumentation to measure various kinds of nuclear radiations. Silicon Carbide (SiC) is among them. In fact, SiC detectors could be used for the on-line measurement of key quantities such as neutron (thermal and fast) and photon fluxes. One main challenge is to enlarge the measurement range of this detector type. The work presented in this paper deals with this aim. Firstly, an introduction dedicated to the use of SiC versus other wide bandgap semiconductors and the characteristics of the studied sensor is shown. Secondly, this paper presents 3D numerical results obtained with a parametrical thermal study of the SiC detector using COMSOL Multiphysics code for a nuclear heating range corresponding to TRIGA nuclear research reactor conditions (integral neutron flux $\sim 2.0 \times 10^{13}$ n·cm$^{-2}$·s$^{-1}$ leading to a nuclear heating rate of 0.25 W·g$^{-1}$ in Tungsten). The main objective is to adapt and optimize the design and the housing of the detector by determining its temperature field for different configurations. The influence of various parameters is presented such as that of the housing material nature, the gas nature around the diode, the gas-gap height and the housing thickness.

## Introduction

Wide bandgap semiconductor materials such as Diamond, Silicon Carbide (SiC), III-V Nitrides or Gallium Arsenide (GaAs) are well-known for their high-power, high-frequency, high-temperature and harsh environment applications. All of this is possible thanks to their lower intrinsic-carrier concentrations than those of Silicon (Si) that induce a very low leakage current. Therefore, these semiconductors are capable of operating at much higher temperature than Si (several hundred degrees). Furthermore, SiC has many advantages in comparison with other wide bandgap semiconductors for measurements in extreme environments. Indeed, it is characterised by a high breakdown-electric field strength, rather high electron mobility, a high thermal conductivity, a high

electron saturation velocity and a high-radiation stability. Moreover, for many years, several improvements were performed about material quality through the development of SiC single crystals with a high-purity and epitaxial layers [1].

In the field of nuclear instrumentation, 4H-SiC is used to build (thermal and/or fast) neutron detectors. They can be based on a $p^+n$ junction diode [2] (cf. Fig. 1). To detect thermal neutrons, a Neutron Converter Layer (NCL) is implanted in a 1 μm thick Aluminum contact. This NCL is composed of a material that has a high thermal neutron absorption cross section such as $^{10}B$ with 3840 barns. The absorption of thermal neutrons by $^{10}B$ leads to the release of charged particles, i.e. $^4He$ nuclei (α particle) and $^7Li$ nuclei. These particles deposit/lose their energy in the successive very thin layers of the semiconductor (from 100 nm to 350 μm) which create electron/hole pairs that are collected by electrodes positioned on both sides of the detector. The sensitive part of the diode is called the Space Charge Region (SCR). Its width depends on the bias voltage applied across the detector and it is located between the 1 μm $p^+$-type epitaxial layer and the n-type epitaxial layer. For this kind of SiC detector, previous original research works have been carried out within the framework of the I_SMART project (Innovative Sensor for Material Ageing and Radiation Testing) involving the CEA and Aix-Marseille University [3]. For instance, for this kind of SiC detector, experimental research work has been carried out on the measurement of thermal neutron fluxes in MINERVE, a Zero-Power Reactor at CEA Cadarache, France with an integral neutron flux (thermal and fast) of 9.41 x$10^8$ n·cm$^{-2}$·s$^{-1}$ [4].
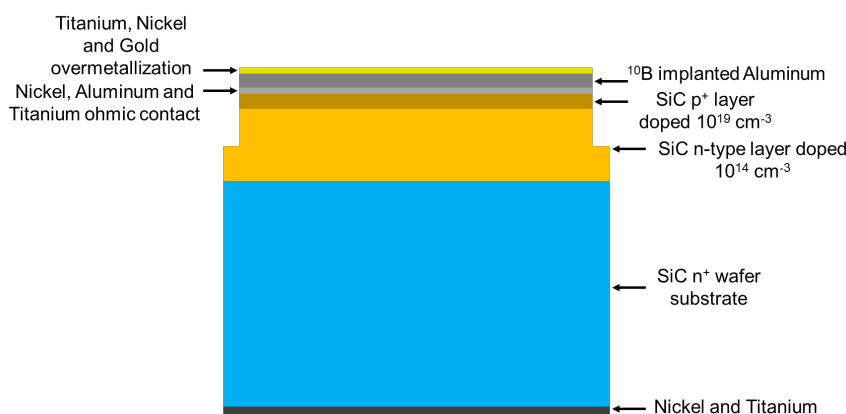


**Figure 1.** Schematic of the 4H-SiC-based diode (see details of thickness in [5])

A new objective is currently being targeted in the framework of the SiC-CALO project (coupling of Silicon Carbide and calorimetric sensors in order to measure key nuclear quantities simultaneously: neutron fluxes and nuclear heating rate). As for the I_SMART project, this new project is also achieved within the framework of a joint laboratory called LIMMEX (Laboratory of Instrumentation and Measurement Methods in EXtreme media) between Aix-Marseille University and the CEA. The project aim is to develop a new type of radiation detection system in order to perform on-line measurements under intense neutron fluxes of 5.5 ×$10^{14}$ n·cm$^{-2}$·s$^{-1}$ for an energy > 1 MeV and high nuclear heating rates up to 20 W·g$^{-1}$ expected in the core of the Jules Horowitz Reactor under construction at the CEA Cadarache research center.

This system will couple a SiC detector with a compact differential calorimeter [5]. To achieve this aim, intermediate steps are necessary. First of all, a new design of each sensor has to be defined thanks to numerical simulations (3D thermal simulations and Monte-Carlo calculations). The optimized design will be manufactured. Then experiments will be carried out in the TRIGA Mark II reactor of the Jožef Stefan Institute (JSI) with a maximum integral neutron flux of about 2.0 x$10^{13}$ n·cm$^{-2}$·s$^{-1}$ and a maximum nuclear heating rate in Tungsten around 0.25 W·g$^{-1}$ in the central irradiation channel [6]. The irradiation campaign will be performed inside an in-core triangular channel (dry air channel) during the first months of 2021. Figure 2 represents the JSI TRIGA Mark II reactor core and shows the various locations of irradiation channels (in yellow) such as the triangular dry air channel also called Triangular Irradiation Channel (TIC). All of these channels can host experiments depending

on the conditions desired (neutron and photon fluxes, nuclear heating rates, temperature, …). The paper focuses on the 3D thermal numerical simulations realized to propose a new sensor design.
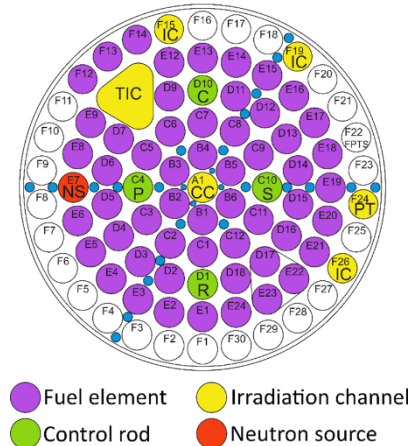


**Figure 2.** Schematic of the core of the Jožef Stefan Institute TRIGA Mark II reactor with the Triangular Irradiation Channel (TIC)

## 3D Thermal Simulation Results

In this part, a parametrical thermal study of various parameters using COMSOL Multiphysics code (finite element code with a heat transfer module) is shown for the SiC detector for a wide range of nuclear heating rate. The nuclear heating rate ($E_n$) represents the energy rate ($J \cdot s^{-1}$), which is released in one gram of matter exposed to nuclear radiation fluxes and corresponds to an increase of the thermal agitation inside the material, which leads to an increase in temperature.

**3D Model.** The presented thermal studies were realized for a system restricted to the SiC detector (the experimental irradiation channel and the coolant fluid flow were not modeled yet). The heat equation is solved with only conductive heat transfers (convective and radiative exchange are neglected inside the detector) and for the stationary state. Moreover, for each component of the system, a heat source ($\rho_i \cdot E_n = Q$) calculated from the nuclear heating rate expected inside the TRIGA reactor ($E_n$) and depending on the material density ($\rho_i$) is applied (cf. Table 1).

**Table 1.** Energy deposition in the detector housing for a nuclear heating rate equal to 0.1 $W \cdot g^{-1}$ and for different materials

| Materials | $\rho_i$ [kg·m$^{-3}$] | Energy deposited Q [W·m$^{-3}$] | Power deposited in the housing P [W] |
|---|---|---|---|
| Aluminun 5754 | 2700 | 270000 | 5.53 |
| Duralumin | 2800 | 280000 | 5.73 |
| Alumina | 3900 | 390000 | 7.98 |
| Titanium TA6V | 4500 | 450000 | 9.21 |
| Stainless Steel 316L | 7850 | 785000 | 16.07 |

Then, the external boundary conditions corresponding to the coolant fluid flow conditions (fluid temperature and induced heat exchange coefficient) are considered. The maximum temperature of the coolant fluid (dry air) is fixed at 40 °C and the heat transfer coefficient related to natural convection is taken from 5 $W \cdot m^{-2} \cdot K^{-1}$ to 25 $W \cdot m^{-2} \cdot K^{-1}$ (only 5 and 10 $W \cdot m^{-2} \cdot K^{-1}$ are presented in this paper). The SiC detector is built in 3D (cf. Fig. 3) for a simplified composition: the housing, the SiC diode, the diode support in Alumina and the gas present in the housing. The two-connection wires and the plugs are not considered.
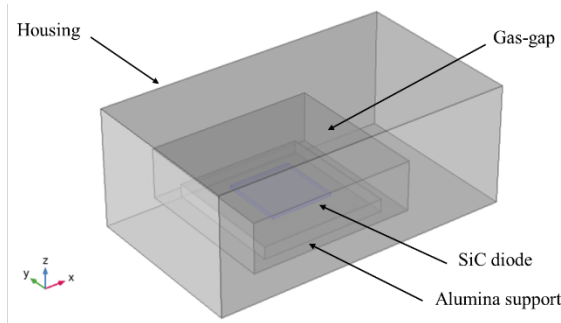
**Figure 3.** Schematic of the detector geometry built with COMSOL Multiphysics

The initial general dimensions of this sensor are presented in Table 2. The mesh sizes used in order to obtain the best compromise between the spatial resolution and the duration of each calculation was an extra-thin mesh. It corresponds to a minimal size equal to 70 µm and a maximal size equal to 1680 µm. This range is sufficient compared to the total height of the SiC diode (a single layer of 371 µm modeled).

**Table 2.** Initial geometrical characteristics of the SiC detector

| Sensor components | Dimensions | | |
|---|---|---|---|
| | Length [mm] | Width [mm] | Height [mm] |
| SiC diode | 10 | 10 | 0.371 |
| Alumina support | 20 | 20 | 2 |
| Housing (external dimensions) | 48 | 28 | 19 |
| Gas-gap | 26.4 | 24 | 8 |

**Results and Interpretations.** The first parameter studied was the effect of the housing material nature on the temperatures reached inside the detector. Five different materials were tested: Aluminum 5754, Duralumin, Alumina, Titanium TA6V and Stainless Steel 316L. Figure 4 gives the induced maximal temperature of the detector versus the nuclear heating rate for these five materials for a heat transfer coefficient equal to 10 $W \cdot m^{-2} \cdot K^{-1}$.
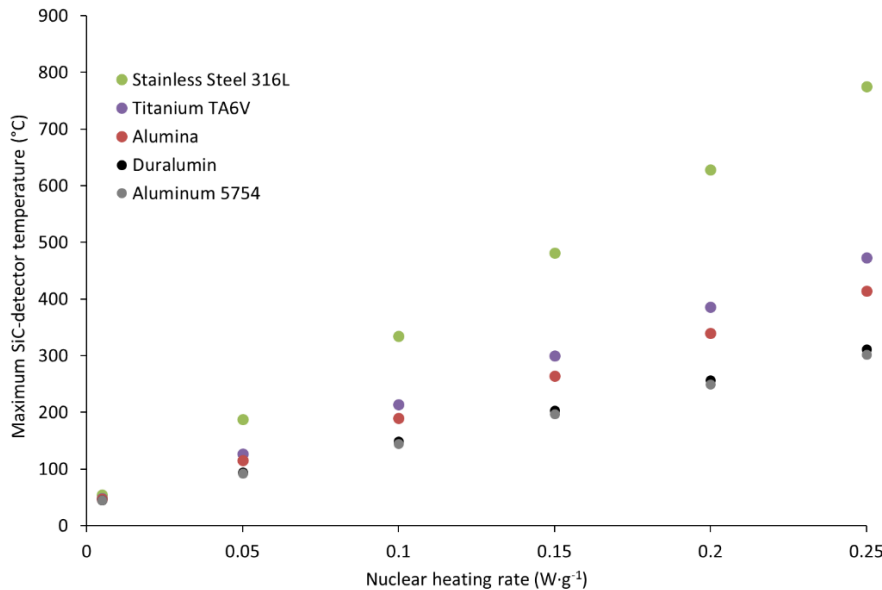
**Figure 4.** Maximum temperature of the SiC detector versus the nuclear heating rate for five housing materials and for a heat transfer coefficient equal to 10 $W \cdot m^{-2} \cdot K^{-1}$ and a fluid temperature equal to 40 °C

As expected, the maximum temperature is obtained for the maximum nuclear absorbed dose rate value (0.25 $W \cdot g^{-1}$) and the greatest material density.

This can be explained through the fact that for a constant volume, the weight of the housing is increasing with the density, so the energy deposited in the system is greater (cf. Table 1), leading to higher temperatures. Figure 5 confirms this behavior. Indeed, this Figure shows the maximum temperature versus the value of the total energy deposition, which depends on the nature of the housing material for a nuclear heating rate equal to 0.1 W·g$^{-1}$. More than 94.6 % of the energy is deposited in the housing. Consequently, a housing made of Duralumin is chosen to achieve lower temperature and thanks to other properties such as its high thermal conductivity, its hardness, its important tensile strength and its ease of machining. An additional advantage is lower residual activation following neutron irradiation.
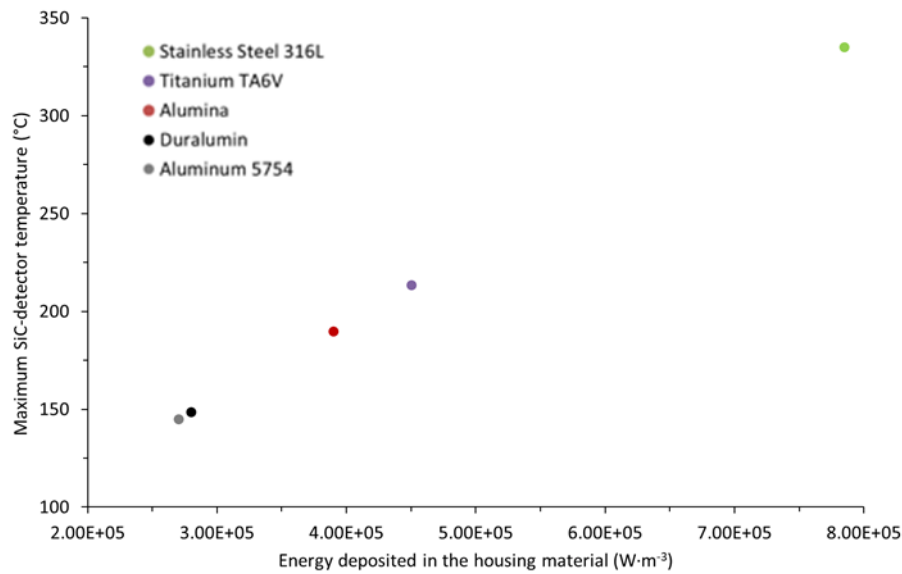


**Figure 5.** Maximum temperature of the SiC detector versus the specific energy deposited in the housing for five housing materials, a heat transfer coefficient equal to 10 W·m$^{-2}$·K$^{-1}$, a fluid temperature equal to 40 °C and for a nuclear heating rate of 0.1 W·g$^{-1}$

The second parameter studied is the gas nature in the gap for a housing made of Duralumin. Five different gases were tested: Air, Nitrogen, Helium, Argon and Xenon. It is observed that the temperatures reached inside the detector are the same for the different gases. A maximum deviation equal to 0.32 °C is observed between the Air and Xenon configurations for a nuclear absorbed dose rate of 0.1 W·g$^{-1}$, a heat transfer coefficient equal to 10 W·m$^{-2}$·K$^{-1}$ and a fluid temperature equal to 40 °C. These low differences can be explained by the fact that, as shown in Figure 6, the major part of the main heat conductive exchange is localized through the Alumina support and the Duralumin housing (the gas acting as a thermal insulator).
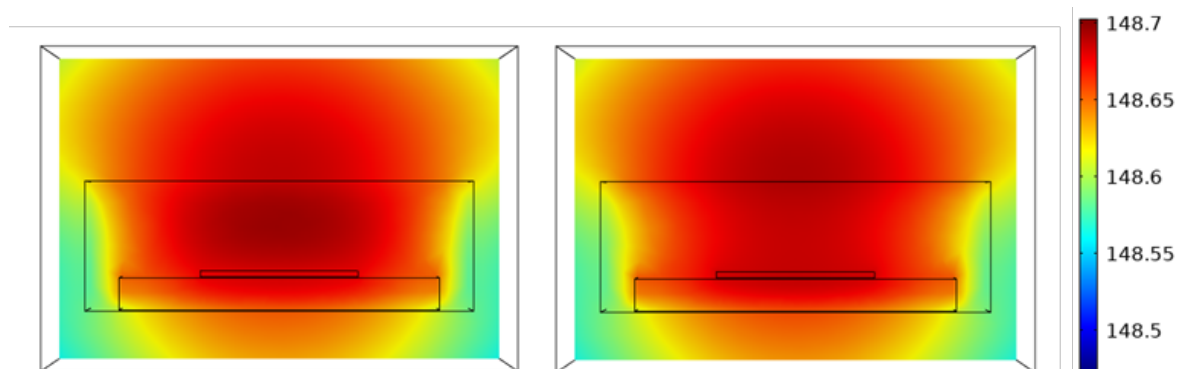


**Figure 6.** Temperature fields (°C) obtained inside the middle of SiC detector with an Air gap (on the left-hand section) and with a Helium gap (on the right-hand section) for a fluid temperature equal to 40 °C, a heat exchange coefficient equal to 10 W·m$^{-2}$·K$^{-1}$ and a nuclear heating rate equal to 0.1 W·g$^{-1}$

It can be concluded that, with this assembly configuration, the gas influence is not significant due to the conductive heat transfer through the Duralumin housing and the Alumina support, which are in contact with no thermal contact resistance considered in the 3D model.

   The third parameter studied was the gas-gap thickness (for a housing made of Duralumin and an Air gap). In fact, the height of the gas-gap was reduced but the housing thickness is kept constant. Figure 7 presents the maximum temperature of the SiC detector versus the gas-gap height for two different values of heat transfer coefficient.
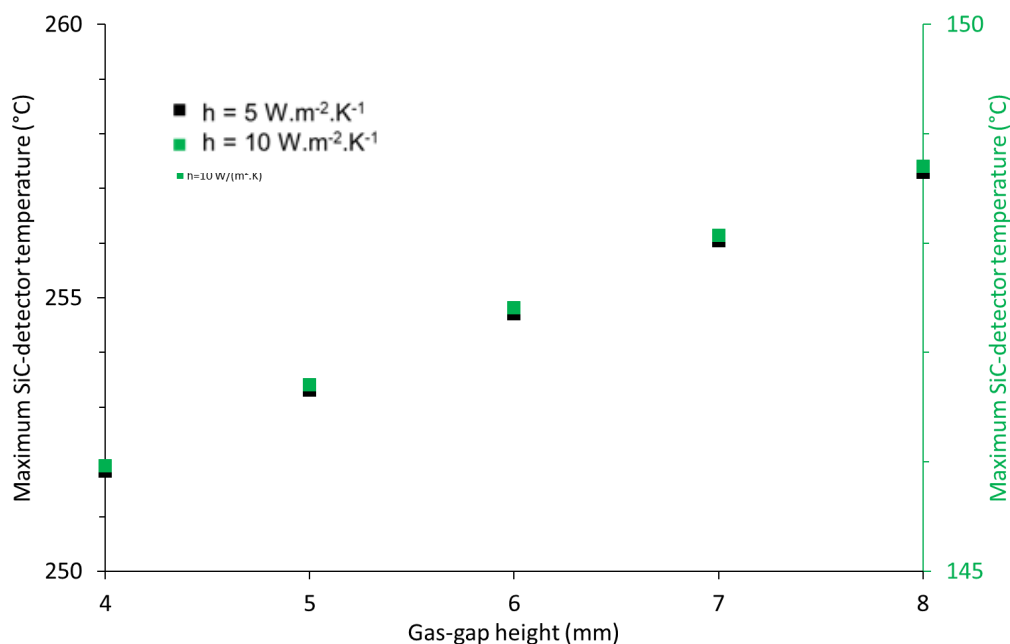


**Figure 7.** SiC detector maximum temperature versus the gas-gap height for two values of heat transfer coefficient, a nuclear heating rate equal to 0.1 $W \cdot g^{-1}$ and a fluid temperature equal to 40 °C

Whatever the applied value of the heat transfer coefficient, the maximum temperature increases with the height of the Air gap. This is due to the increasing of the housing volume and consequently of the total energy deposition. Actually, between the two extreme values of gas height, there is an increase of 0.8 W of power deposited on matter (13.14 %). In addition, when the heat transfer coefficient increases, the temperature of the detector decreases significantly. Whatever the gas-gap height, the variation of the temperature is around -107.3 °C for a heat transfer coefficient of 10 $W \cdot m^{-2} \cdot K^{-1}$ instead of 5 $W \cdot m^{-2} \cdot K^{-1}$.



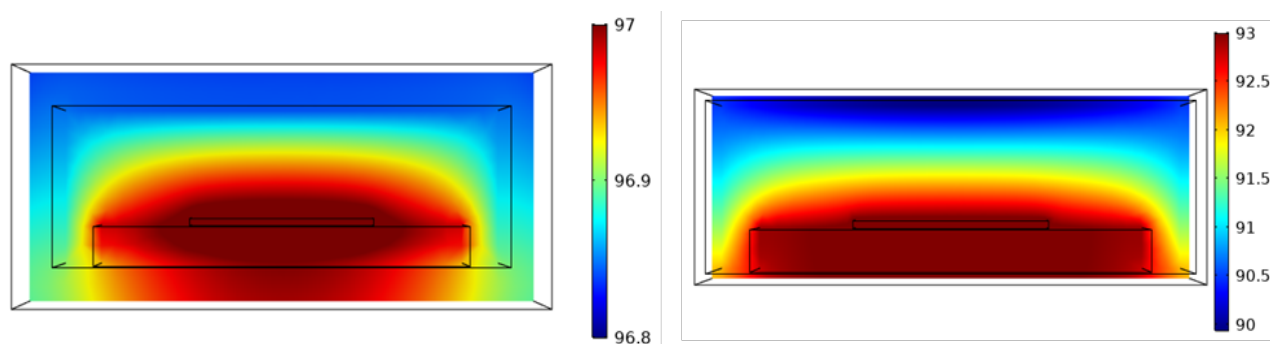**Figure 8.** Temperature fields (°C) obtained for the 2 mm Duralumin housing (on the left-hand section) and the 0.5 mm Stainless Steel housing (on the right-hand section) with a fluid temperature equal to 40 °C, a heat exchange coefficient equal to 10 $W \cdot m^{-2} \cdot K^{-1}$ and a nuclear heating rate equal to 0.1 $W \cdot g^{-1}$

The last parameter investigated in this thermal study was the thickness of the housing for two different materials: 2 mm in Duralumin and 0.5 mm in Stainless Steel 316L respectively. For these two configurations, the thickness of the encapsulation is the same in all directions and the gas-gap retains its original dimensions (cf. Table 2). Figure 8 represents the temperature fields obtained with a fluid temperature equal to 40 °C, a heat exchange coefficient equal to 10 $W \cdot m^{-2} \cdot K^{-1}$ and a nuclear heating equal to 0.1 $W \cdot g^{-1}$ for the Duralumin (on the left-hand section) and for the Stainless Steel (on the right-hand section) configurations. These two configurations lead to a significant decrease in the temperature (lower than 100 °C) in comparison with the previous dimensions of the detector due to the decrease of the thickness of the housing that induces a lower energy deposition in matter. The similar thermal behavior associated to the two configurations is due to the applied reduction of the housing thickness, which depends on the material nature.

**Conclusion**

Thanks to a parametric thermal study, various conclusions were obtained to optimize the SiC detector design. For the first parameter, corresponding to the housing material nature, it was confirmed that the temperature increases in the detector when the nuclear heating rate and the density of the material increase. This is due to the higher energy deposition in the matter. Consequently, a housing made of Duralumin was chosen. Regarding the second parameter (the gas nature in the gap around the SiC diode and its support), the influence is not significant due to its thermal insulation coupled to the predominant conductive heat transfer through the Alumina support and the part of the Duralumin housing in contact with it. In the case of the third parameter (the gas-gap height), when it decreases, the maximum temperature is lower due to the diminution of the housing volume and consequently of the total energy deposition. This thermal behavior is reinforced for a higher heat transfer coefficient applied. For the last parameter studied, the thickness of the housing for a 2 mm Duralumin housing and a 0.5 mm Stainless Steel housing, an important temperature decrease was obtained as consequence of a lower energy deposition in matter. For these two cases, the maximum temperature reached agrees with the use of Tin alloy welds with a melting temperature above 200 °C ensuring the wire connection.

In the future, a more detailed 3D model with the SiC detector in the triangular dry air channel of the Jožef Stefan Institute TRIGA Mark II reactor will be carried out. This model will contain also other components such as connectors, screws and the instrumentation cables. Moreover, it will consider thermal radiative transfer and specific heat transfer coefficient values using suited natural convection correlation formula depending on the heat sources. Another relevant Monte-Carlo particle transport simulation and modeling dedicated to the interactions between nuclear radiations and matter will be realized. These numerical studies and the results obtained will be used to define the most optimized device for the JSI irradiation campaign scheduled next year. Later, in order to estimate the discrepancy between experimental and numerical results for a specific point inside the detector, a nuclear-radiation hardened thermocouple will be integrated close to the SiC diode inside the gas-gap.

**References**

[1] V. V. Buniatyan and V. M. Aroutiounian, Wide gap semiconductor microwave devices, J. Phys. D: Appl. Phys. 40 (2007) 6355-6385.

[2] F. Issa, V. Vervisch, L. Ottaviani, D. Szalkai, L. Vermeeren, A. Lyoussi, A. Kuznetsov, M. Lazar, A. Klix, O. Palais, R. Ferone, A. Hallén, Study of the stability of 4H-SiC detectors by thermal neutron irradiation, Materials Science Forum 821-823 (2015) 875-878.

[3] A. Lyoussi, et al., I_SMART a collaborative project on Innovative Sensor for Material Ageing and Radiation Testing: European Innovative Project for SiC applications in harsh media. KIC_Innoenergy, "CCAV," I_SMART Proposal/Exhibit 1 (2012).

[4]  O. Obraztsova, L. Ottaviani, B. Geslot, G. de Izarra, O. Palais, A. Lyoussi, W. Vervisch, Comparison between Silicon-Carbide and Diamond for Thermal neutron detection at Room Temperature, IEEE Transactions on Nuclear Science 67, No. 5, (2020) 863-871.

[5]  V. Valero, A. Volte, L. Ottaviani, A. Lyoussi, M. Carette, J. Brun, C. Reynard-Carette, Parametrical study for the coupling of a silicon carbide (SiC) detector and a calorimeter to measure simultaneously neutron flux and radiation absorbed dose rate in research reactors, RRFM 2020 conference proceedings (2020).

[6]  K. Ambrožič, G. Žerovnik, L. Snoj, Computational analysis of the dose rates at JSI TRIGA reactor irradiation facilities, Applied Radiation and Isotopes 130, (2017) 140-152.